

A Comparative Study of CART and PTM for Modelling Water Age

WANG Haiyan¹⁾, GUO Xinyu²⁾, LIU Zhe^{1), *}, and GAO Huiwang¹⁾

1) Key Laboratory of Marine Environment and Ecology, Ministry of Education, Ocean University of China, Qingdao 266100, P. R. China
2) Center for Marine Environmental Studies, Ehime University, Matsuyama 790-8577, Japan

(Received May 9, 2013; revised May 30, 2013; accepted November 6, 2014)

© Ocean University of China, Science Press and Springer-Verlag Berlin Heidelberg 2015

Abstract CART (Constituent-oriented age and residence time theory) and PTM (Particle-tracking method) are two widely used numerical methods to calculate water age. These two methods are essentially equivalent in theory but their results may be different in practice. The difference of the two methods was evaluated by applying them to calculate water age in an idealized one-dimensional domain. The model results by the two methods are consistent with each other in the case with either spatially uniform flow field or spatially uniform diffusion coefficient. If we allow the spatial variation in horizontal diffusion, a term called pseudo displacement arising from the spatial variation of diffusion coefficient likely plays an important role for the PTM to obtain accurate water age. In particular, if the water particle is released at a place where the diffusion is not the weakest, the water age calculated by the PTM without pseudo displacement is much larger than that by the CART. This suggests that the pseudo displacement cannot be neglected in the PTM to calculate water age in a realistic ocean. As an example, we present its potential importance in the Bohai Sea where the diffusion coefficient varies spatially and greatly.

Key words CART; PTM; pseudo displacement; water age

1 Introduction

Advection and diffusion are two important processes in coastal material transport. The material transport time-scales play an important role in the algal bloom (Hilton *et al.*, 1998). Because of the complex spatiotemporal structure of coastal currents, it is helpful to define auxiliary variables, such as water age, to understand the material transport processes in coastal zone of oceans (Zimmerman, 1976; Takeoka, 1984; Deleersnijder *et al.*, 2001; Monsen *et al.*, 2002; Delhez *et al.*, 2004). Water age is defined as the time elapsed since the departure of a water particle from an area, where its age is prescribed to be zero, to its arrival at a water body of interest (Bolin and Rodhe, 1973; Takeoka, 1984).

Numerical simulation is one of the major methods for studying water age. Compared with other methods (*i.e.*, field observations and theoretical study), numerical simulation can consider both advection and diffusion processes in a realistic ocean with complex topography and forcing conditions. Therefore, numerical simulation is widely used in calculating mean water age (Chen, 2007; Wang *et al.*, 2010; Liu *et al.*, 2011; de Brye *et al.*, 2013;

Liu *et al.*, 2012). The mean water age is defined as the mass-weighted arithmetic average of the ages of all of the water particles within a target domain.

Among the aforementioned studies on mean water age, constituent-oriented age and residence time theory (CART, www.climate.be/cart) (Deleersnijder *et al.*, 2001) and particle-tracking method (PTM) (Zhang, 1995) are two widely used methods. For instance, Wang *et al.* (2010) studied the mean age of Changjiang River water and de Brye *et al.* (2013) studied the mean age of canal and dock water by the CART; Chen (2007) studied the mean age of Alafia River water and Liu *et al.* (2011) studied the mean age of the Tahan Stream, Hsintien Stream, and Keelung River water by the PTM; Liu *et al.* (2012) used both the CART and PTM to investigate the mean age of Yellow River water in the Bohai Sea.

The CART obtains mean water age by solving two Eulerian equations. As a Lagrangian method, the PTM traces water particles along their pathways and records their ages as time passes. These two methods are essentially equivalent in theory (Liu *et al.*, 2012). However, the mean water age calculated by the CART and PTM may be different in practice (Liu *et al.*, 2012). In order to propose some useful suggestions for studying mean water age in a realistic ocean with two methods, the difference of the two methods was evaluated by applying them to an idealized one-dimensional channel in this study.

* Corresponding author. Tel: 0086-532-66786568
E-mail: zliu@ouc.edu.cn

2 Model Description

2.1 CART Model

To calculate mean water age $a(t, x, y, z)$ using the CART (Deleersnijder *et al.*, 2001), two equations need to be solved for the concentration $C(t, x, y, z)$ and age concentration $\beta(t, x, y, z)$ of the targeted water particles, respectively. The concentration $C(t, x, y, z)$ is controlled by Eq. (1).

$$\frac{\partial C}{\partial t} = - \left[\frac{\partial(uC)}{\partial x} + \frac{\partial(vC)}{\partial y} + \frac{\partial(wC)}{\partial z} \right] + \left[\frac{\partial}{\partial x} (K_H \frac{\partial C}{\partial x}) + \frac{\partial}{\partial y} (K_H \frac{\partial C}{\partial y}) + \frac{\partial}{\partial z} (K_V \frac{\partial C}{\partial z}) \right], \quad (1)$$

where t is time; x, y and z are three coordinates in space; u, v and w are velocities in x, y and z directions, respectively; K_H and K_V are horizontal and vertical diffusion coefficients, respectively.

The age concentration $\beta(t, x, y, z)$ is calculated by Eq. (2).

$$\frac{\partial \beta}{\partial t} = C - \left[\frac{\partial(u\beta)}{\partial x} + \frac{\partial(v\beta)}{\partial y} + \frac{\partial(w\beta)}{\partial z} \right] + \left[\frac{\partial}{\partial x} (K_H \frac{\partial \beta}{\partial x}) + \frac{\partial}{\partial y} (K_H \frac{\partial \beta}{\partial y}) + \frac{\partial}{\partial z} (K_V \frac{\partial \beta}{\partial z}) \right]. \quad (2)$$

After solving Eqs. (1) and (2), the mean water age $a(t, x, y, z)$ is calculated as the ratio of $\beta(t, x, y, z)$ to $C(t, x, y, z)$:

$$a = \beta / C. \quad (3)$$

2.2 PTM Model

The PTM module (Zhang, 1995) used in this study is from estuarine and coastal ocean model coupled with a sediment transport module (ECOMSED) (Blumberg, 2002). The three coordinates (x, y, z) of a particle in this module was controlled by Eq. (4).

$$\begin{cases} x(t + \Delta t) - x(t) = \xi \sqrt{2K_H \Delta t} + \frac{\partial K_H}{\partial x} \Delta t + u \Delta t \\ y(t + \Delta t) - y(t) = \xi \sqrt{2K_H \Delta t} + \frac{\partial K_H}{\partial y} \Delta t + v \Delta t, \\ z(t + \Delta t) - z(t) = \xi \sqrt{2K_V \Delta t} + \frac{\partial K_V}{\partial z} \Delta t + w \Delta t \end{cases} \quad (4)$$

where Δt is time step; ξ is random number with zero mean and unit variance.

The second term on right hand side of Eq. (4) represents pseudo displacement arising from spatial variation in diffusion.

For a particle released at time t_0 , its position is given by Eq. (4) and its age is $t - t_0$. The mean water age (t, x, y, z) is the average of all the particles' age at location (x, y, z) at time t .

2.3 Model Configuration

We considered a one-dimensional finite domain (signed as x direction) with a length L of 20 km. In the PTM and CART, we used the same grid interval Δx (=200 m) and time step Δt (=10 s).

In the one-dimensional domain, the governing Eqs. (1)–(3) in the CART can be simplified to

$$\frac{\partial C}{\partial t} = - \frac{\partial(uC)}{\partial x} + \frac{\partial}{\partial x} (K \frac{\partial C}{\partial x}), \quad (5)$$

$$\frac{\partial \beta}{\partial t} = C - \frac{\partial(u\beta)}{\partial x} + \frac{\partial}{\partial x} (K \frac{\partial \beta}{\partial x}), \quad (6)$$

$$a(t, x) = \frac{\beta(t, x)}{C(t, x)}, \quad (7)$$

where K is the diffusion coefficient.

The initial values of concentration $C(t, x)$ and age concentration $\beta(t, x)$ were both set to 0 in the whole domain. At the releasing point ($x=x_r$), the concentration $C(t, x)$ was always set to 1, that is, the water particle was released continuously at $x=x_r$. The age concentration at $x=x_r$ was set to 0, resulting in a zero age of water particle at $x=x_r$ (Bolin and Rodhe, 1973; Takeoka, 1984). At the two ends ($x=0$ and $x=L$), the concentration $C(t, x)$ and age concentration $\beta(t, x)$ both were set to 0, indicating that the water particle could not re-enter the model domain.

In the PTM, the Eq. (4) can be simplified as:

$$x(t + \Delta t) - x(t) = \xi \sqrt{2K \Delta t} + \frac{\partial K}{\partial x} \Delta t + u \Delta t. \quad (8)$$

To better understand the movement of a particle, the terms $\sqrt{2K \Delta t}$, $\frac{\partial K}{\partial x} \Delta t$ and $u \Delta t$ were defined as characteristic diffusion displacement Δx_{Dif} , pseudo displacement Δx_{Pse} , and advection displacement Δx_{Adv} , respectively.

In the PTM, the initial and boundary conditions were the same as those in the CART. In the experiments for temporally varied flow field (Section 3.2.2), 1 particle was released at $x=x_r$ at each time step within the first period of temporally varied velocity (T). In other experiments, a total of 1000 particles were released at $x=x_r$ at the first time step. When a particle was released at $x=x_r$, its age was set to be 0. Subsequently, the particle age was updated at every time step until it reached the end of the domain ($x=0$ or $x=L$), where the particle was excluded from the model.

We recorded the positions of all the particles released in the first period of temporally varied velocity during the total time of calculation. It should be pointed out that the period in the numerical experiments for constant velocity (in all Sections except Section 3.2.2) could be considered as Δt . For calculating the mean water age in a steady state, we need not only the pathways of the particles released in the first period, but also those in the second period and

succeeding periods. Based on the fact that the velocity field and diffusivity coefficients used for the PTM calculation were repeated at the same time in every period, we assumed that the particles released in the second and succeeding periods have the same pathways as those released in the first period. The only difference is in the ages of the particles. In this manner, we obtained the pathways of the particles released after the second period without additional PTM calculations. This counting method for mean water age has been used for the mean age of Yellow River water in the Bohai Sea (Liu *et al.*, 2012).

We stopped the calculation when the mean water age did not change with time in the CART and PTM and therefore obtained the mean water age results in a steady state.

To better understand the mean water age distribution in a steady state, the age frequency distribution function was calculated based on the results of the PTM. The age frequency distribution function $\varphi(\tau, x)$ is defined by Eq. (9) (Bolin and Rodhe, 1973), *i.e.*,

$$\varphi(\tau, x) = \frac{1}{M_0(x)} \frac{dM(\tau, x)}{d\tau}, \tag{9}$$

where, $M_0(x)$ is the total number of particles at x ; $M(\tau, x)$ is the total number of the particles whose age is smaller than or equal to an age τ at x .

To represent the relative mass of water particles between location x and releasing location x_r in a steady state, R is defined by Eq. (10):

$$R(x) = M^*(x) / M^*(x_r). \tag{10}$$

In the CART, $M^*(x)$ and $M^*(x_r)$ are the concentration at x and x_r , respectively; in the PTM, $M^*(x)$ and $M^*(x_r)$ are the particle number at x and x_r , respectively.

3 Results

Because advection and diffusion are two important processes controlling material transport in coastal water, we examine the mean water age distribution controlled by them. In previous studies on mean water age by the PTM, the displacement of a particle usually contains only Δx_{Dif} and Δx_{Adv} (Chen, 2007; Liu *et al.*, 2011) but does not contain Δx_{Pse} . Hence, in addition to the comparison of the CART and PTM, we also pay some attention to the difference between the mean water ages calculated by the PTM with and without Δx_{Pse} , respectively.

3.1 Diffusion

3.1.1 Constant and uniform diffusion coefficient

If the model only includes constant and uniform diffusion coefficient without advection, the analytical solution for mean water age can be found in Appendix A in Liu *et al.* (2012). In this study, $x_r = 0.25L$; the mean water age is given by Eq. (11):

$$a(x) = \frac{x^* l}{6K} \left(2 - \frac{x^*}{l} \right), \tag{11}$$

where at $x \geq 0.25L$, $x^* = x - 0.25L$, $l = 0.75L$; at $x < 0.25L$, $x^* = 0.25L - x$, $l = 0.25L$.

In the case of $K = 20 \text{ m}^2 \text{ s}^{-1}$, Fig.1a (black line) shows that mean water age is zero at x_r and increases as a parabolic function to the distance away from x_r . The mean water age calculated by the CART and PTM both agrees well with the analytical solution (Fig.1a).

There is one major peak of frequency at approximately 0 in the age frequency distribution function for the area around x_r (*i.e.*, $x = 0.3L$) (Fig.1b, red line; Fig.1d). This peak corresponds to the young water particles that quickly spread into this area from x_r . In addition to these young water particles, we can also identify the presence of old water particles that have an age longer than 5 d (Fig.1b, red line), indicating that the water particles return to $x = 0.3L$ from the area outside $x = 0.3L$. Therefore, the mean water age of about 3 d at $x = 0.3L$ (Fig.1a) results from the coexistence of newly released water particles from x_r and the returned water particles from the area outside $x = 0.3L$.

The age frequency distribution function shows a more complex composition of mean water age in the region far away from x_r (*i.e.*, $x = 0.7L$) (Fig.1c, red line) than that in the region around x_r (*i.e.*, $x = 0.3L$, Fig.1b, red line). There is one major peak of frequency at approximately 10 d in the age frequency distribution function at $x = 0.7L$ (Fig.1c, red line; Fig.1d). This peak corresponds to the water particles that directly spread into this area from x_r . However, the frequency at approximately 5–20 d in the age frequency distribution function at $x = 0.7L$ is not much smaller than that at approximately 10 d (Fig.1c, red line). As a result of coexistence of such water particles, the mean water age at $x = 0.7L$ is about 18 d (Fig.1a).

Fig.1e is the extension of results at $x = 0.3L$ and $x = 0.7L$ to the whole model domain (*i.e.*, $x > 0.25L$). At any location x in the model domain, there are both water particles with small age and water particles with large age. The mean water age at x is a result of coexistence of all the water particles at x (Fig.1a). Similar to the mean water age, the age corresponds to the max. frequency in the age frequency distribution function increases as a parabolic function to the distance away from the x_r (Fig.1d).

In the above experiments, we also changed the values of K but the agreement of the mean water age between the CART and PTM was kept. Apparently, the agreement between two methods is independent of K .

3.1.2 Spatially varied diffusion coefficient

We used a spatially varied diffusion coefficient controlled by Eq. (12) (Fig.2a):

$$K(x) = K_0 + A \cos(2\pi x / L), \quad x \in [0, L], \tag{12}$$

where, $K_0 = 20 \text{ m}^2 \text{ s}^{-1}$, $A = 15 \text{ m}^2 \text{ s}^{-1}$.

According to Eq. (8), the displacement of a particle contains Δx_{Dif} (Fig. 2b, black line) and Δx_{Pse} (Fig.2b, red line). Δx_{Pse} is smaller than Δx_{Dif} in this case (Fig.2b). Δx_{Pse} is positive at $x > 0.5L$ while negative at $x < 0.5L$ (Fig.2b, red line). Therefore, Δx_{Pse} helps the particle move towards to

two ends of the channel.

According to Eq. (12), the minimum diffusion coefficient occurs at $x=0.5L$ (Fig.2a). Fig.3a shows that the mean water age by the PTM with Δx_{pse} is almost the same as that by the PTM without Δx_{pse} when the releasing point is $0.5L$ ($x_r=0.5L$). Both of them agree well with the mean water age by the CART. The mean water age is zero at x_r and increases as a parabolic function to the distance away from x_r . However, if the releasing point changes to $0.25L$ ($x_r=0.25L$), the mean water age by the CART agrees well with that by the PTM with Δx_{pse} , but is much smaller than that by the PTM without Δx_{pse} at $x>0.25L$ (Fig.3c). This is consistent with the results reported by Visser (1997) that the PTM with only Δx_{Dif} causes the particles to gather in low diffusion regions. As a result, it is difficult for the particles to leave the low diffusion region ($x=0.5L$) (Fig.3d, blue line), and the mean water age at $x>0.25L$ becomes much longer (Fig.3c, blue line) than that calculated by the CART. As Δx_{pse} is considered in the PTM, it helps the water particles leave the low diffusion region and move towards $x=0$ or $x=L$ (Fig.3d, red line).

It must be noted that in the case of $x_r=0.5L$, the PTM without Δx_{pse} also gather water particles in the low diffusion region ($x=0.5L$) (Fig.3b, blue line). However, in this

case Δx_{pse} is significantly smaller than Δx_{Dif} (Fig.2b) and it is Δx_{Dif} that determines the displacement of water particles. In addition, since $x=0.5L$ is also the releasing point of water particles, the age there is always set to be zero according to the boundary condition. Therefore, the mean water ages by the PTM with and without Δx_{pse} are almost the same (Fig.3a).

In the case of $x_r=0.25L$, one major peak at approximately 5 d can be found in the age frequency distribution function at $x=0.5L$ (Figs.4a, b). This peak indicates that whether the PTM contains Δx_{pse} or not, a certain number of water particles spend approximately 5 d spreading into this area from x_r . However, the frequency at approximately 5 d in the age frequency distribution function at $x=0.5L$ by the PTM without Δx_{pse} is smaller than that by the PTM with Δx_{pse} (Fig.4a). On the other hand, the frequency at longer than 30 d in the age frequency distribution function at $x=0.5L$ by the PTM without Δx_{pse} is larger than that by the PTM with Δx_{pse} (Fig.4a). This indicates again that in the calculation of PTM without Δx_{pse} , compared with the calculation of PTM with Δx_{pse} , it is difficult for the water particles to leave the low diffusion region ($x=0.5L$) (Fig.3d, blue line) with a longer mean water age at $x>0.25L$ (Fig.3c).

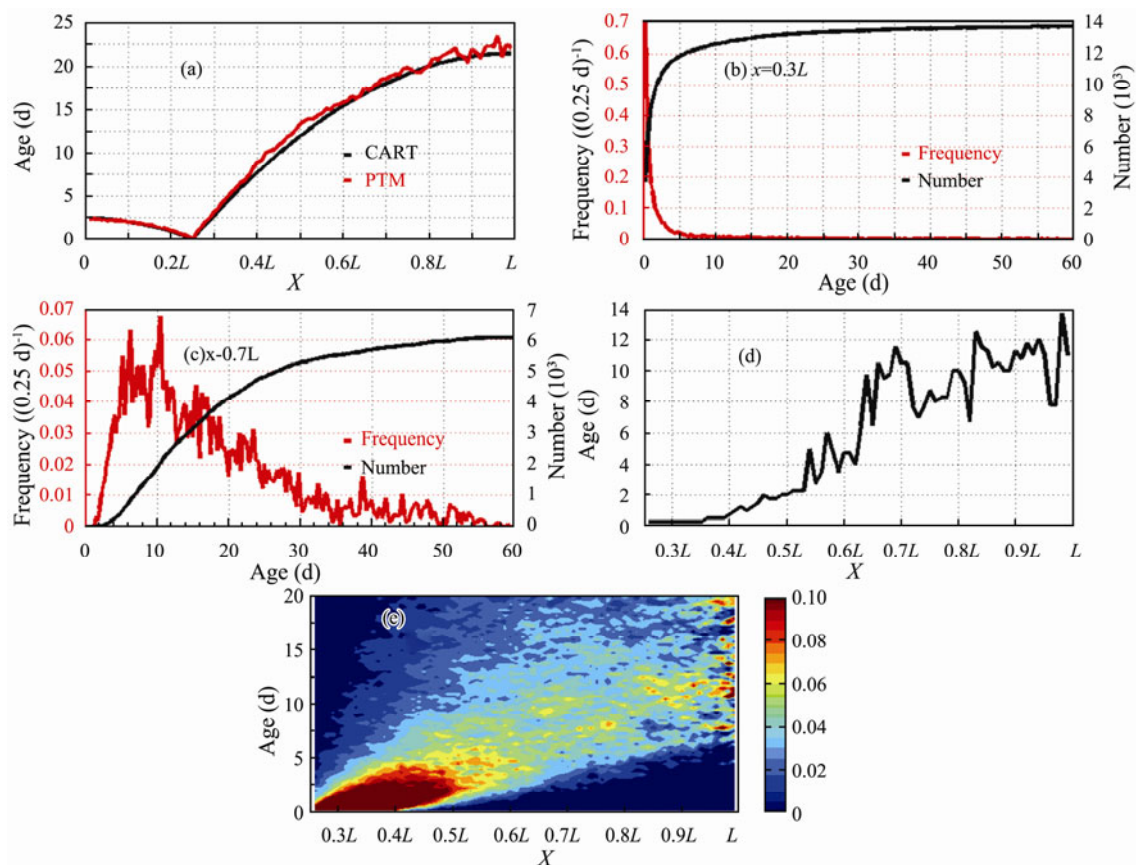


Fig.1 The diffusion coefficient is constant and uniform ($20\text{ m}^2\text{ s}^{-1}$) and water particle is released at $0.25L$ ($x_r=0.25L$). (a) Comparison of mean water ages by CART (black line), PTM (red line), and analytical solution. The analytical solution of Eq. (11) is overlapped by CART (black line). (b) Total number (black line, *i.e.*, $M(\tau, x)$ in Eq. (9)) and age frequency distribution function (red line, *i.e.*, $\varphi(\tau, x)$ in Eq. (9)) at $x=0.3L$. The age range (τ) is limited to 60 d since the frequency of particles with age longer than 60 d is too small to be identified. (c) The same as Fig.1(b), but for $x=0.7L$. (d) The age corresponds to the maximum of frequency distribution function at $x>0.25L$. (e) The age frequency distribution function $\varphi(\tau, x)$ (unit: $(0.25\text{ d})^{-1}$) at $x>0.25L$. The age range (τ) is limited to 20 d.

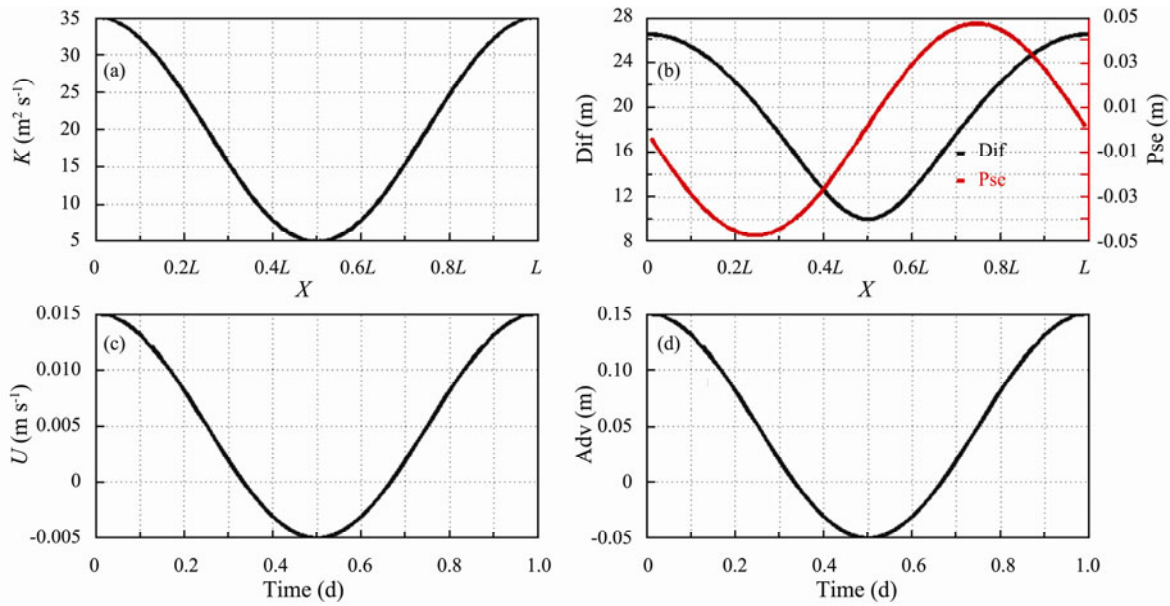


Fig.2 (a) The distribution of spatially varied diffusion coefficient by Eq. (12). (b) Based on the diffusion coefficient shown in Fig.2(a), Δx_{Dif} (black line) and Δx_{Pse} (red line) calculated by Eq. (8). (c) The distribution of temporally varied velocity by Eq. (13). (d) Based on the velocity shown in Fig.2(c), Δx_{Adv} calculated by Eq. (8). See Section 2.3 for the definitions of Δx_{Dif} , Δx_{Pse} , and Δx_{Adv} .

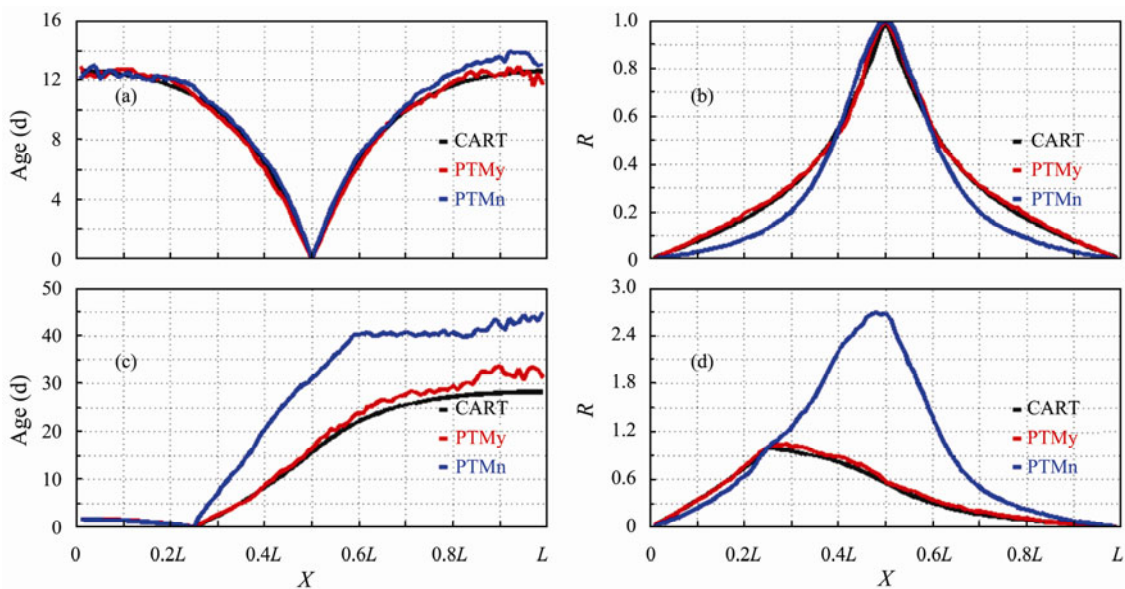


Fig.3 The spatially varied diffusion coefficient is controlled by Eq. (12). (a) Water particle is released at $0.5L$ ($x_r=0.5L$). Comparison of mean water ages by CART (black line), PTM with Δx_{Pse} (red line), and PTM without Δx_{Pse} (blue line). (b) Water particle is released at $0.5L$ ($x_r=0.5L$). Comparison of R (defined by Eq. (10)) by CART (black line), PTM with Δx_{Pse} (red line), and PTM without Δx_{Pse} (blue line). (c) The same as Fig.3(a), but for $x_r=0.25L$. (d) The same as Fig.3(b), but for $x_r=0.25L$.

Figs.4c and 4d are the extension of results at $x=0.5L$ to the whole model domain (*i.e.*, $x>0.25L$) by the PTM with and without Δx_{Pse} , respectively. At any location x , the frequency at small age by the PTM without Δx_{Pse} is smaller than that by the PTM with Δx_{Pse} (Figs.4c and 4d), while the frequency at large age by the PTM without Δx_{Pse} is larger than that by the PTM with Δx_{Pse} (Fig.4c, Fig.4d). As a result, the mean water age by the PTM without Δx_{Pse} is significantly larger than that by the PTM

with Δx_{Pse} (Fig.3c). Similar to mean water age, the ages corresponding to the max. frequencies by the PTM with and without Δx_{Pse} both increase as a parabolic function to the distance away from the x_r (Fig.4b). The age corresponding to the max. frequency by the PTM without Δx_{Pse} is slightly longer than that by the PTM with Δx_{Pse} (Fig.4b).

In summary, in the case of spatially varied diffusion coefficient, the PTM should include Δx_{Pse} .

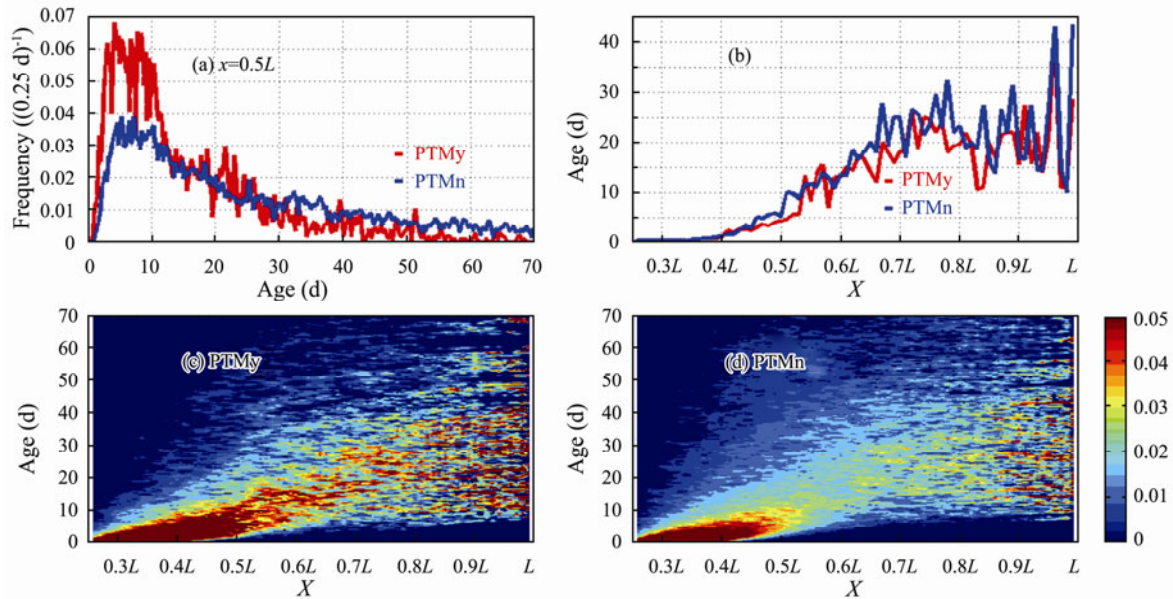


Fig.4 The spatially varied diffusion coefficient is controlled by Eq. (12) and water particle is released at $0.25L$ ($x_r=0.25L$). (a) The age frequency distribution function $\varphi(\tau, x)$ at $x=0.5L$ by PTM with Δx_{pse} (red line) and by PTM without Δx_{pse} (blue line). (b) The age corresponds to the maximum of frequency distribution function at $x>0.25L$ by PTM with Δx_{pse} (red line) and by PTM without Δx_{pse} (blue line). (c) The age frequency distribution function $\varphi(\tau, x)$ (unit: $(0.25 \text{ d})^{-1}$) for $x>0.25L$ by PTM with Δx_{pse} . (d) The same as Fig.4(c), but for PTM without Δx_{pse} . The age range (τ) in Figs.4(a), 4(c), and 4(d) is limited to 70 d.

3.2 Advection

3.2.1 Constant and uniform velocity

In the case of constant and uniform velocity (u) without diffusion, the analytical solution for mean water age is x/u , where x is the distance away from x_r . Assuming $u=0.005 \text{ m s}^{-1}$ and $x=0.25L$, we show the analytical solution in Fig.5a, in which the mean water age is zero at x_r and increases linearly with the distance away from the x_r . The mean water age obtained by the CART and PTM agrees well with the analytical solution (Fig.5a). From the age frequency distribution function, each particle's age equals to the mean age at any location x in the model domain.

3.2.2 Temporally varied velocity

In this case, we assume a temporally varied velocity given by Eq. (13) (Fig.2c):

$$u(t) = u_0 + B \cos(2\pi t / T), \quad (13)$$

where $u_0=0.005 \text{ m s}^{-1}$, $B=0.01 \text{ m s}^{-1}$, $T=86400 \text{ s}$.

According to Eq. (8), in the case of temporally varied velocity without diffusion, the displacement of a particle contains only Δx_{Adv} (Fig.2d). Again, we released particles at $x_r=0.25L$.

Fig.5b shows that the mean water age by the PTM and CART both are zero at x_r at $t=105.5 \text{ d}$. The mean water age by the PTM increases linearly with the distance away from the x_r , with a small fluctuation. The mean water age by the CART also increases linearly with the distance away from the x_r , but with little fluctuation. The PTM

deals with each particle and is capable of considering the internal information (*e.g.*, uneven age of particles) inside a grid. The exchange of particles between neighboring grids can be well described in the PTM. However, the uniformity of age of particles within each grid cannot be considered in Eqs. (5)–(6) for CART.

At $t=105.5 \text{ d}$, there is one major peak of frequency at approximately 1.7 d in the age frequency distribution function for the area around x_r (*i.e.*, $x=0.3L$) (Fig.5c, red line; Fig.5e). This peak corresponds to the young water particles that spread quickly into this area from x_r . In addition to these young water particles, we can also identify the presence of old water particles that have an age longer than 2.3 d (Fig.5c, red line), indicating that the water particles can return to $x=0.3L$ from the area outside $x=0.3L$ because of the negative velocity (Fig.2c). As the case of diffusion, the mean water age (about 2 d) at $x=0.3L$ (Fig.5b) is a result of coexistence of newly released water particles from x_r and the returned water particles from the area outside $x=0.3L$.

The age frequency distribution function shows a more complex composition of mean water age in the region far away from x_r (*i.e.*, $x=0.7L$) (Fig.5d, red line) than that in the region around x_r (*i.e.*, $x=0.3L$, Fig.5c, red line). For instance, there are two major peaks of frequency at approximately 20.6 d and 20.9 d in the age frequency distribution (Fig.5d, red line). As a result of coexistence of the water particles with different ages, the mean water age at $x=0.7L$ is about 21 d (Fig.5b).

Fig.5f is the extension of results at $x=0.3L$ and $x=0.7L$ to the whole model domain (*i.e.*, $x>0.25L$). At any location x in the model domain, there are water particles with

both small and large ages. The mean water age at x is a result of coexistence of all the water particles at x (Fig.5b). Compared with the age frequency distribution function under diffusion (Figs.1e, 4c, and 4d), the age of frequency distribution function under advection (Fig.5f) presents a smaller range. Similar to the mean water age, the age cor-

responding to the max. frequency in the age frequency distribution function increases linearly with the distance away from the x_r , with a very small fluctuation (Fig.5e).

In summary, in the case of temporally varied velocity, the mean water age by the PTM and CART agrees well with each other.

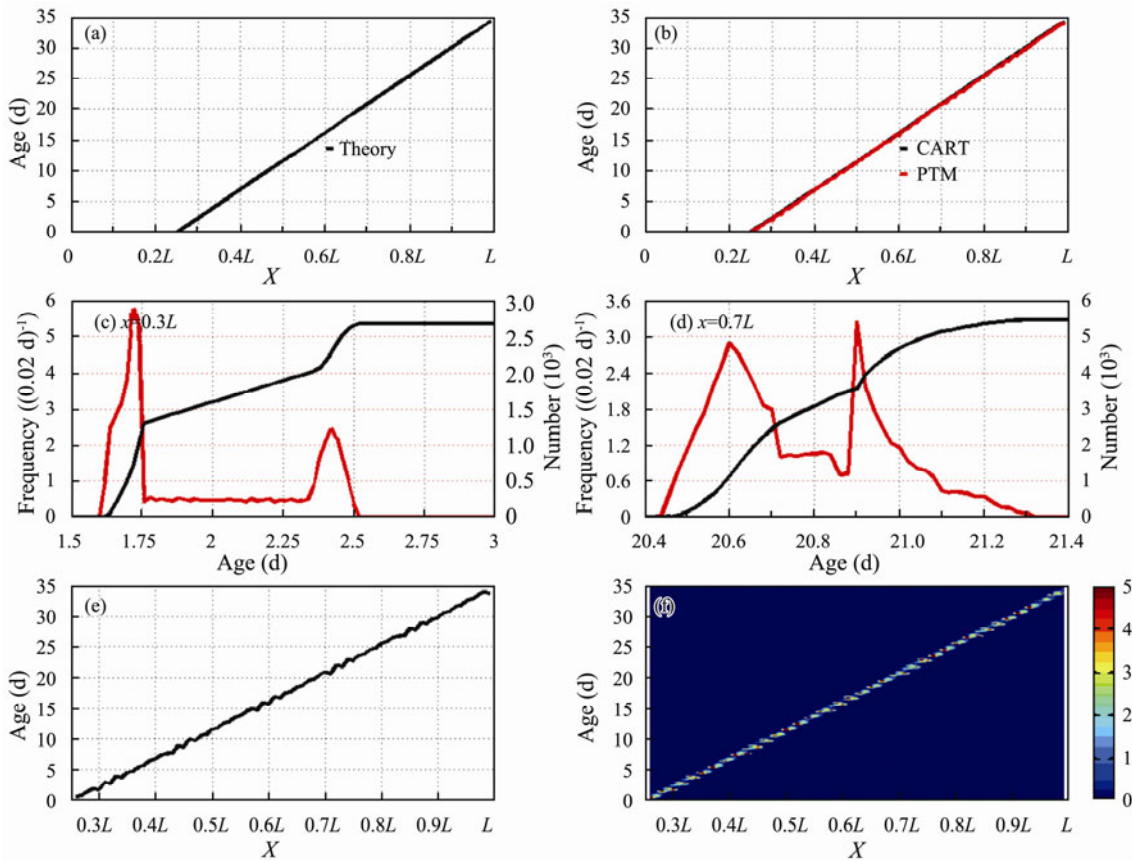


Fig.5 Water particle is released at $0.25L$ ($x_r=0.25L$). (a) The analytical solution for mean water age (x/u , where x is the distance away from x_r) with a constant and uniform velocity (0.005 m s^{-1}). The mean water ages by CART and PTM overlap with the analytical solution. (b) Comparison of mean water ages by CART (black line) and PTM (red line) with temporally varied velocity controlled by Eq. (13). (c) Total number (black line, $M(\tau, x)$ in Eq. (9) of the particles with ages less than or equal to an age (τ) at $x=0.3L$; age frequency distribution function (red line, $\varphi(\tau, x)$ in Eq. (9) at $x=0.3L$. The age range (τ) is from 1.5 to 3 d. (d) The same as Fig.5(c), but for $x=0.7L$. The age range (τ) is from 20.4 to 21.4 d. (e) The age corresponds to the maximum of frequency distribution function at $x > 0.25L$. (f) The age frequency distribution function $\varphi(\tau, x)$ (unit: $(0.02 \text{ d})^{-1}$) at $x > 0.25L$. The age range (τ) is limited to 35 d. Same as Fig.5(b), the temporally varied velocity is controlled by Eq. (13) in Figs.5(c)–5(f). Figs. 5(b)–5(f) are at time $t=105.5$ d.

4 Discussion

4.1 The Disappearance of the Mean Water Age Difference Between the CART and PTM Without Δx_{pse} in the Case of the Spatially Varied Diffusion Coefficient

The several experiments we discussed above show that the mean water age results by the CART and PTM generally agree well with each other except for that in the case of spatially varied diffusion coefficient (Section 3.1.2). In that case, if the water particle was not released at the place with weakest diffusion, the mean water age by the CART is much smaller than that by the PTM without Δx_{pse} (Fig.3c). The cause for this inconsistency is because

the PTM without Δx_{pse} collects water particles in low diffusion region (Fig.3d).

From Eq. (12), the average magnitude of gradient of spatially varied diffusion coefficient (*i.e.*, $|\partial K/\partial x|$) is about $3 \times 10^{-3} \text{ m s}^{-1}$ at $x > 0.25L$. In order to calculate the average of $|\partial K/\partial x|$ at $x > 0.25L$, we first calculate the magnitude of gradient of spatially varied diffusion coefficient ($|\partial K/\partial x|$) at each location x at $x > 0.25L$. The average of $|\partial K/\partial x|$ at $x > 0.25L$ is the arithmetic average of all the $|\partial K/\partial x|$ at $x > 0.25L$.

It is of interests to know under what circumstances the phenomenon that the mean water age by the CART is smaller than that by the PTM without Δx_{pse} at $x > 0.25L$ (Fig.3c) will vanish along with the reduction in $|\partial K/\partial x|$.

We used a spatially varied diffusion coefficient given

by Eq. (14) to examine this problem.

$$K(x) = K_0 + A \cos(2\pi x / L), x \in [0, L], \quad (14)$$

By changing value of A in Eq. (14) to 10, 8, 6.5, 5.5, and $5 \text{ m}^2 \text{ s}^{-1}$, we obtained the average of $|\partial K / \partial x|$ as 2×10^{-3} , 1.6×10^{-3} , 1.3×10^{-3} , 1.1×10^{-3} , and $1 \times 10^{-3} \text{ m s}^{-1}$ at $x > 0.25L$, respectively.

Again, we assumed $x_r = 0.25L$. When $|\partial K / \partial x|$ decreases, the mean water age difference between the CART and PTM without Δx_{pse} at $x > 0.25L$ decreases gradually (Fig.6). When the average of $|\partial K / \partial x|$ is $1 \times 10^{-3} \text{ m s}^{-1}$, the mean water age by the CART is almost the same as that by the PTM without Δx_{pse} (Fig.6e). In this case, no matter the PTM includes Δx_{pse} or not, there is one major peak of frequency at about 5 d in the age frequency distribution function at $x = 0.5L$ (Fig.7a), being the same as in the case where the average of $|\partial K / \partial x|$ is $3 \times 10^{-3} \text{ m s}^{-1}$ (Fig.4a). The frequency at about 5 d and longer than 30 d by the PTM without Δx_{pse} at $x = 0.5L$ is almost the same as that by the PTM with Δx_{pse} (Fig.7a). In the whole domain, the age corresponding to the maximum frequency (Fig.7b) and the age frequency distribution function (Figs.7c, d) by the PTM without Δx_{pse} is almost the same as that by the PTM with Δx_{pse} . These features are not found in the results when the average of $|\partial K / \partial x|$ is $3 \times 10^{-3} \text{ m s}^{-1}$ (Fig.4). Therefore, it is likely that the problem that the mean water age

by the CART is smaller than that by the PTM without Δx_{pse} at $x > 0.25L$ will vanish, if the magnitude of gradient of spatially varied diffusion coefficient decreases to a certain value (*i.e.*, the average of $|\partial K / \partial x|$ not larger than $1 \times 10^{-3} \text{ m s}^{-1}$).

On the other hand, advection and diffusion coexist in the realistic ocean. It is therefore necessary to examine the impact of velocity on the PTM without Δx_{pse} in spatially varied diffusion domain. In the next experiments, besides the diffusion coefficient given by Eq. (12), a constant and uniform velocity is added at $x \geq 0.25L$. In Figs.8a, 8b, 8c, and 8d, the velocity is set to 0.0015, 0.005, 0.015, and 0.05 m s^{-1} , respectively. Again, we assumed $x_r = 0.25L$.

According to Eq. (8), the displacement of a particle contains Δx_{dif} , Δx_{pse} , and Δx_{adv} at $x \geq 0.25L$. Here, to show the relative importance of Δx_{pse} and Δx_{adv} , a parameter R^* is defined in Eq. (15):

$$R^* = \left| \frac{\Delta x_{\text{pse}}}{\Delta x_{\text{adv}}} \right| = \left| \frac{\partial K}{u \partial x} \right|. \quad (15)$$

The average of R^* equals to 2, 0.67, 0.2, and 0.067 in Figs.8a–8d, respectively. In order to calculate the average of R^* for $x > 0.25L$, we first calculate R^* at each location x for $x > 0.25L$. The average of R^* for $x > 0.25L$ is the arithmetic average of all the R^* for $x > 0.25L$.

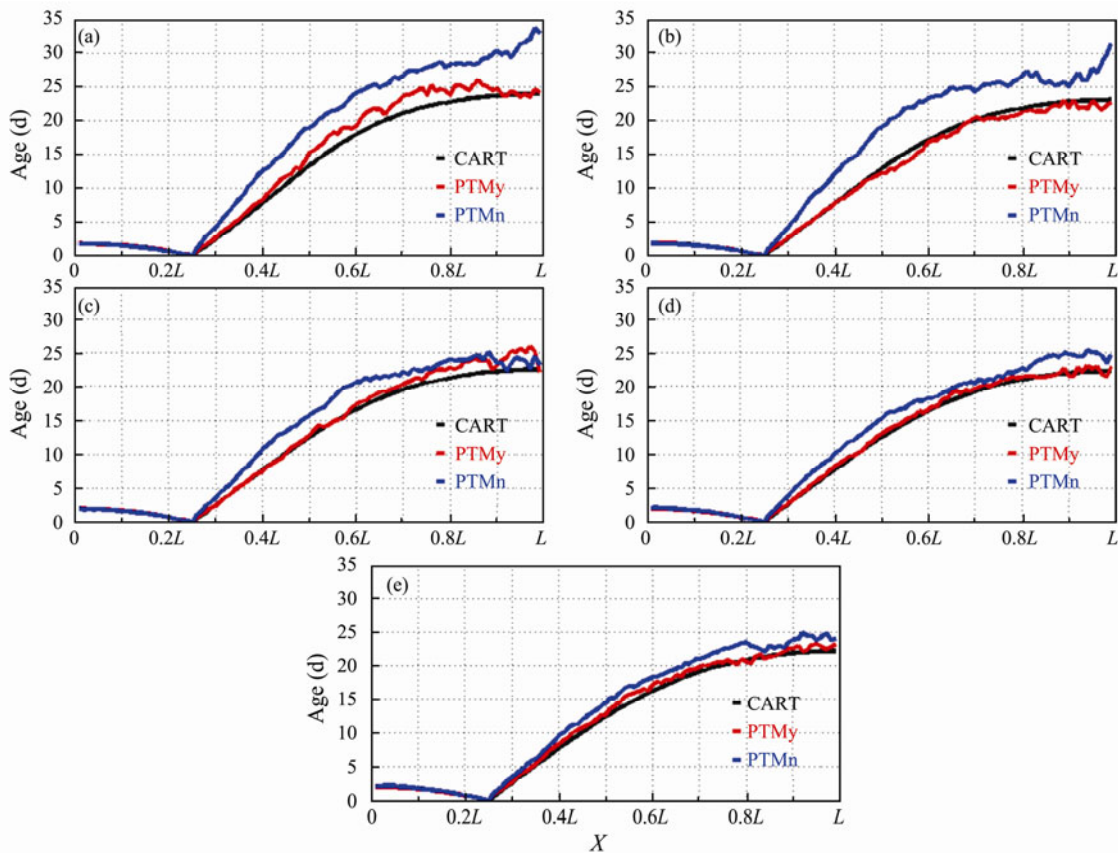


Fig.6 Water particle is released at $0.25L$ ($x_r = 0.25L$). (a) Comparison of mean water ages by CART (black line), PTM with Δx_{pse} (red line), and PTM without Δx_{pse} (blue line) with spatially varied diffusion coefficient controlled by Eq. (14) when A is set to $10 \text{ m}^2 \text{ s}^{-1}$. (b)–(e) The same as Fig.6(a), but for spatially varied diffusion coefficient controlled by Eq. (14) when A is set to 8, 6.5, 5.5, and $5 \text{ m}^2 \text{ s}^{-1}$, respectively.

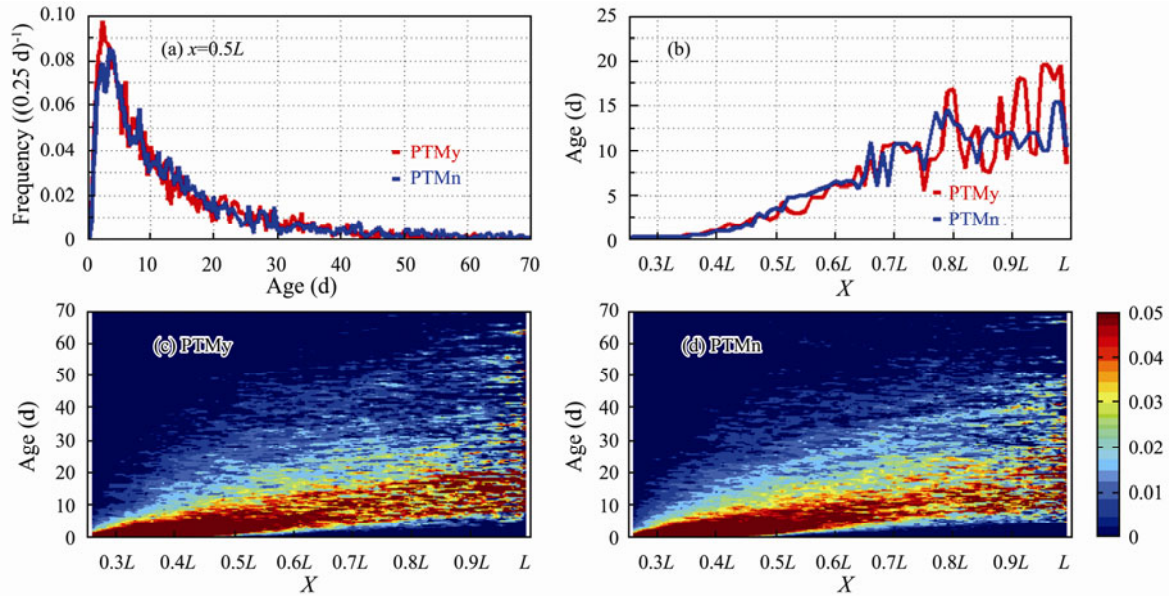


Fig.7 The same as Fig.4, but for spatially varied diffusion coefficient controlled by Eq. (14) when A is set to $5 \text{ m}^2 \text{ s}^{-1}$. Water particle is released at $0.25L$ ($x_r=0.25L$).

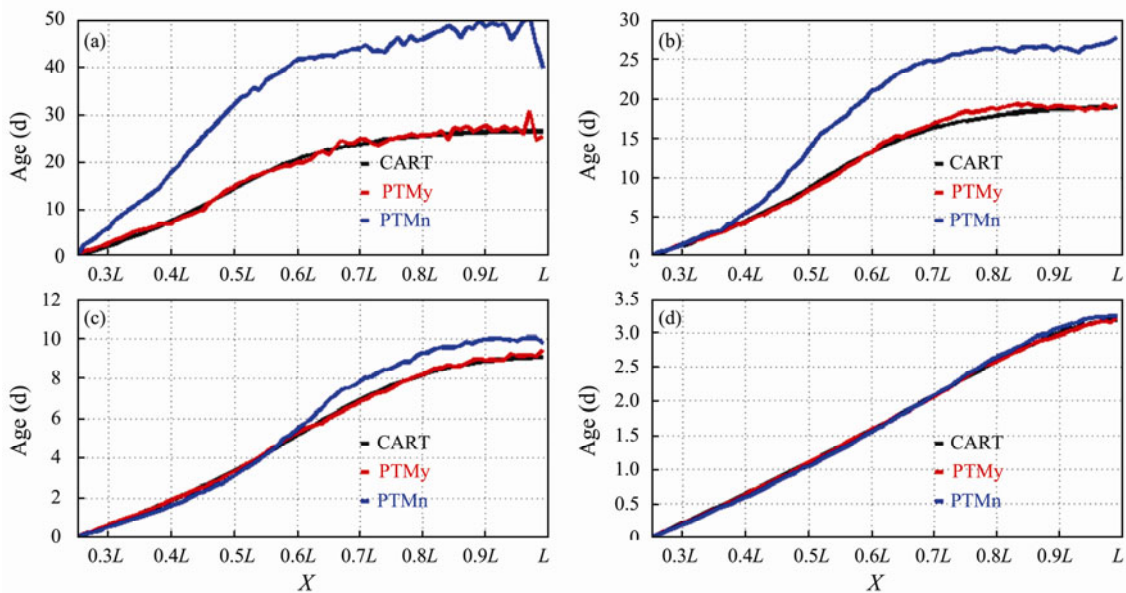


Fig.8 Water particle is released at $0.25L$ ($x_r=0.25L$). (a) Comparison of mean water ages between those by CART (black line), PTM with Δx_{pse} (red line), and PTM without Δx_{pse} (blue line). The spatially varied diffusion coefficient is controlled by Eq. (12) and a constant and uniform velocity (0.0015 m s^{-1}) is added for $x \geq 0.25L$. (b)–(d) The same as Fig.8(a), but the velocities are set to 0.005 , 0.015 , and 0.05 m s^{-1} , respectively.

For R^* values, the mean water age by the CART agrees well with those calculated by the PTM with Δx_{pse} (Fig.8, red and black lines). Regarding the PTM without Δx_{pse} , the agreement is not kept for some values of R^* . For instance, the mean water age by the CART is much shorter than that by the PTM without Δx_{pse} when the average of R^* is 2 (Fig.8a). In this case, advection is too weak to cover up the mean water age difference caused by spatially varied diffusion coefficient (Fig.3c). In the calculation of the PTM without Δx_{pse} , it is difficult for water particles to leave the low diffusion region ($x=0.5L$) and therefore a lot of water particles gather there (Fig.3d).

In the case with both advection and diffusion, even as

the average of R^* decreases to 0.67 (Fig.8b) and 0.2 (Fig.8c), the mean water age by the CART is still shorter than that by the PTM without Δx_{pse} . However, compared with Fig.8a, the mean water age difference between the CART and PTM without Δx_{pse} greatly decreases. The mean water age by the CART agrees well with that by the PTM without Δx_{pse} when the average of R^* is 0.067 (Fig.8d). In this case, advection is strong enough to cover up the age difference caused by spatially varied diffusion coefficient. Therefore, if the velocity increases to a certain extent (*i.e.*, the average of R^* not larger than 0.067), the phenomenon that the mean water age by the CART is shorter than that by the PTM without Δx_{pse} at $x > 0.25L$

will vanish.

4.2 Application to the Realistic Ocean

In this section, we take the Bohai Sea as an example to study the application of CART and PTM to a realistic ocean. The Bohai Sea is a semi-enclosed water body with an average depth of 18 m. It is divided into 5 subregions, namely Laizhou Bay, Bohai Bay, Liaodong Bay, the central Basin, and Bohai Strait. The major rivers that flow into the Bohai Sea include the Yellow River, the Haihe River, the Luanhe River, and the Liaohe River (Fig.9).

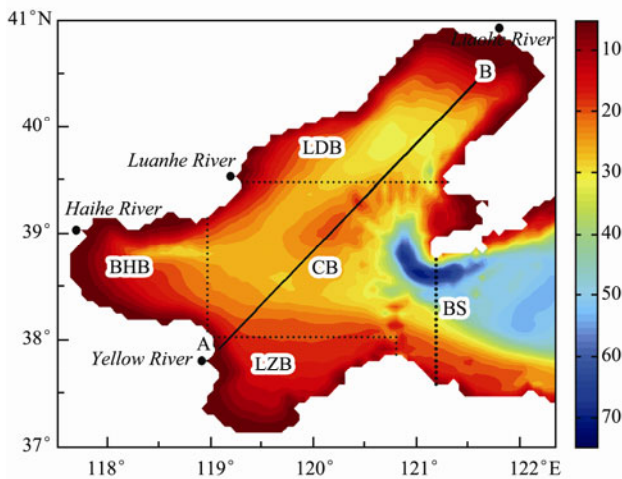


Fig.9 Bathymetry of the Bohai Sea (unit: m). The Bohai Sea is divided into 5 subregions: Laizhou Bay (LZB), Bohai Bay (BHB), Liaodong Bay (LDB), the central basin (CB), and Bohai Strait (BS). The black dots represent the locations of the river mouths of the Yellow River, the Haihe River, the Luanhe River, and the Liaohe River, respectively. Line AB denotes the section along which vertical diffusion coefficient is given in Fig.10b.

The diffusion coefficient and velocity used here were calculated by the model validated by Wang *et al.* (2008). The horizontal resolution was 1/18 degree in both the zonal and meridional directions. In the vertical direction, 21 sigma levels were distributed (0.000, -0.002, -0.004, -0.010, -0.020, -0.040, -0.060, -0.080, -0.100, -0.120, -0.140, -0.170, -0.200, -0.300, -0.400, -0.500, -0.650, -0.800, -0.900, -0.950, and -1.000). The spatial variability of horizontal diffusion coefficient (λ_1), the ratio of the spatial variability of horizontal diffusion coefficient to the horizontal velocity (λ_2), the spatial variability of vertical diffusion coefficient (λ_3), and the ratio of the spatial variability of vertical diffusion coefficient to the vertical velocity (λ_4) are calculated by Eqs. (16)–(19), respectively:

$$\lambda_1 = \sqrt{\left(\frac{\partial K_H}{\partial x}\right)^2 + \left(\frac{\partial K_H}{\partial y}\right)^2}, \tag{16}$$

$$\lambda_2 = \sqrt{\left(\frac{\partial K_H / u}{\partial x}\right)^2 + \left(\frac{\partial K_H / v}{\partial y}\right)^2}, \tag{17}$$

$$\lambda_3 = \left| \frac{\partial K_V}{\partial z} \right|, \tag{18}$$

$$\lambda_4 = \left| \frac{\partial K_V / w}{\partial z} \right|. \tag{19}$$

We interpolated K_V at equal distance in the vertical direction before calculating λ_3 and λ_4 by Eq. (18) and Eq. (19).

The annual K_H for the surface layer of the Bohai Sea (Fig.10a) shows that the K_H is higher in the coastal area (*i.e.*, estuaries, $>40 \text{ m}^2 \text{ s}^{-1}$) than in the offshore area (*i.e.*, the central basin, $<20 \text{ m}^2 \text{ s}^{-1}$). The distribution of K_H (Fig.10a) induces a high λ_1 in the coastal area (*i.e.*, estuaries, $>0.003 \text{ m s}^{-1}$) in the surface layer of Bohai Sea (Fig.10c). λ_1 is small in the offshore area (*i.e.*, the central basin, about 0.002 m s^{-1}) and it is even less than 0.001 m s^{-1} in some areas (Fig.10c). Apparently, the magnitude of gradient of spatially varied horizontal diffusion coefficient is smaller in the offshore area than in the coastal area. According to the analysis for the spatially varied diffusion coefficient in Section 3.1.2 and Section 4.1, the Δx_{pse} cannot be neglected in the PTM to calculate mean water age when the magnitude of gradient of spatially varied diffusion coefficient is larger than 0.001 m s^{-1} . The λ_2 for the surface layer of the Bohai Sea (Fig.10e) shows that λ_2 is larger in the coastal area (*i.e.*, estuaries, >0.2) than in the offshore area (*i.e.*, the central basin, <0.2). This indicates that the impact of horizontal advection compared with horizontal diffusion is stronger in the offshore area than in the coastal area. According to the analysis for the spatially varied diffusion coefficient with constant and uniform velocity in Section 4.1, Δx_{pse} should be considered in the PTM when R^* (indicating the effect of diffusion coefficient and velocity in one-dimensional domain) is not less than 0.2. If we consider the effects of both horizontal diffusion coefficient and horizontal velocity in the Bohai Sea, the PTM should include Δx_{pse} at least for the coastal area (*i.e.*, estuaries) of the Bohai Sea in the horizontal direction.

The annual K_V along transect AB in the Bohai Sea (Fig.10b, location being shown in Fig.9) shows that the K_V is smaller for the surface layer (*i.e.*, shallower than 5 m) than in the middle and bottom layers (*i.e.*, deeper than 10 m). The distribution of K_V (Fig.10b) induces a higher λ_3 in the surface layer (*i.e.*, shallower than 5 m, $>0.003 \text{ m s}^{-1}$) than in the middle and bottom layers (*i.e.*, deeper than 10 m, about 0.002 m s^{-1}) (Fig.10d). In some areas, λ_3 is even less than 0.001 m s^{-1} (Fig.10d). This indicates that the magnitude of gradient of spatially varied vertical diffusion coefficient is smaller in the middle and bottom area than in the surface area. According to the analysis for the spatially varied diffusion coefficient in Section 3.1.2 and Section 4.1, the Δx_{pse} cannot be neglected in the PTM to calculate mean water age when the magnitude of gradient of spatially varied diffusion coefficient is larger than 0.001 m s^{-1} . Fig.10f shows that the λ_4 is very large for the whole Bohai Sea ($>10^2$) because the vertical velocity is extremely small, indicating that the impact of vertical

advection compared with vertical diffusion is very small in the whole Bohai Sea. Hence, it is necessary for the PTM to consider Δx_{Pse} in the vertical direction for the

whole Bohai Sea.

In summary, the PTM must include Δx_{Pse} for the realistic shallow waters (*e.g.*, the Bohai Sea).

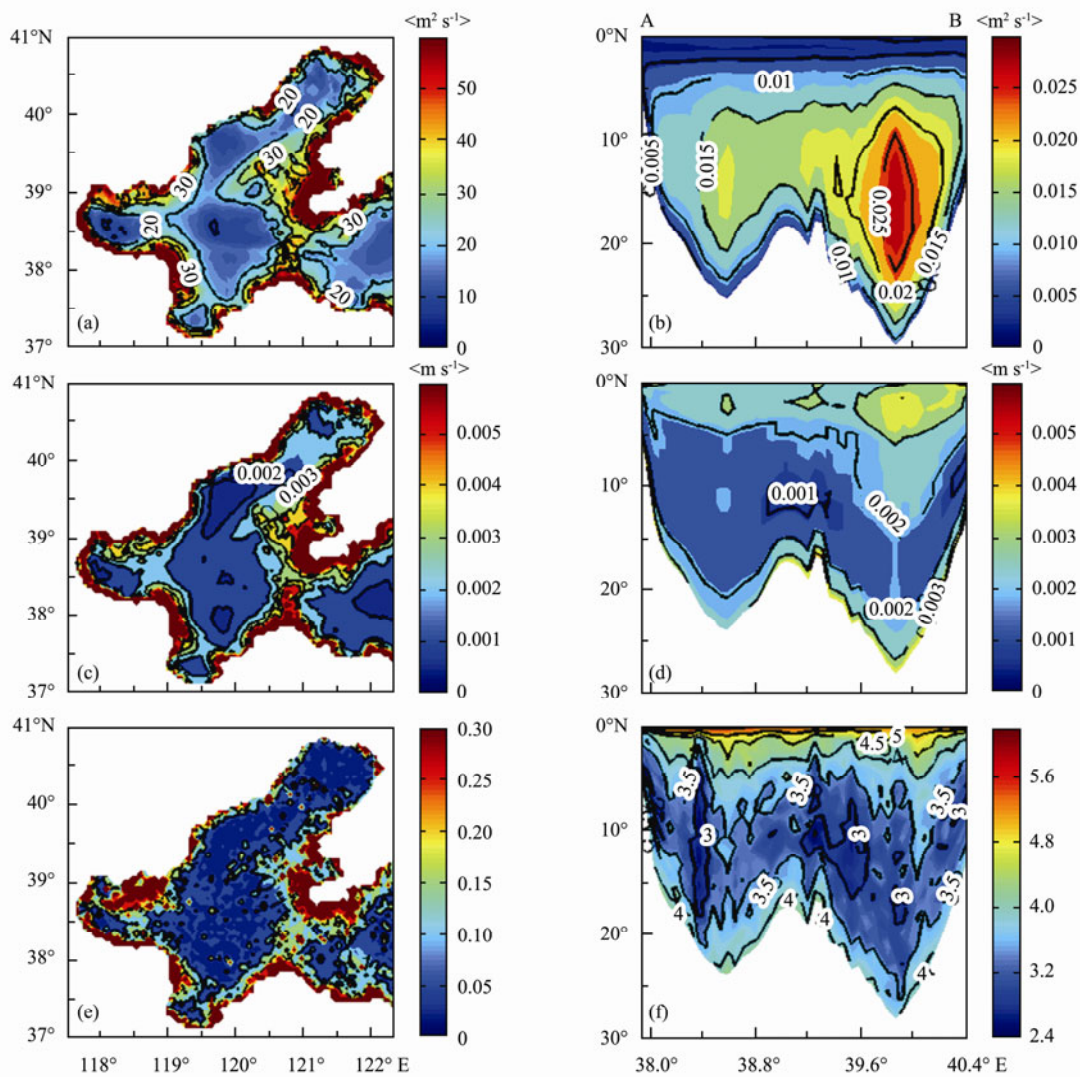


Fig.10 (a) The annual horizontal diffusion coefficient for the surface layer (1 m) of the Bohai Sea. The contour interval is $10 \text{ m}^2 \text{ s}^{-1}$. (b) The annual vertical diffusion coefficient along transect AB (location is shown in Fig.9). The contour interval is $0.005 \text{ m}^2 \text{ s}^{-1}$. (c) Based on the horizontal diffusion coefficient shown in Fig.10(a), the spatial variability of horizontal diffusion coefficient (λ_1) calculated by Eq. (16). The contour interval is 0.001 m s^{-1} . (d) Based on the vertical diffusion coefficient shown in Fig.10(b), the spatial variability of vertical diffusion coefficient (λ_3) is calculated by Eq. (18). The contour interval is 0.001 m s^{-1} . (e) Based on the horizontal diffusion coefficient shown in Fig.10(a), the ratio of the spatial variability of horizontal diffusion coefficient to the horizontal velocity (λ_2) is calculated by Eq. (17). The contour interval is 0.1. (f) Based on the vertical diffusion coefficient shown in Fig.10(b), the ratio of the spatial variability of vertical diffusion coefficient to the vertical velocity (λ_4) is calculated by Eq. (19). The contour interval is 0.5. Colors represent the common logarithm of λ_4 .

5 Summary

The difference in mean water age given by the CART and PTM was studied in an idealized one-dimensional computation domain. The model results by the two methods are consistent with each other in the case with either spatially uniform flow field or spatially uniform diffusion coefficient. In the case with a spatially varied diffusion coefficient, the mean water ages given by the

CART and PTM with Δx_{Pse} agree well with each other. If the water particle is released where the diffusion is weakest, the mean water ages given by the CART and PTM without Δx_{Pse} also agree well with each other. If the water particle is released at other places, the mean water age by the CART is much shorter than that by the PTM without Δx_{Pse} . If the magnitude of gradient of spatially varied diffusion coefficient decreases to a certain extent, this difference decreases. The difference also decreases along with the increasing of velocity. As a general conclusion,

we recommend that the PTM should include the pseudo displacement caused by the spatial variation in the horizontal and vertical diffusion in a realistic sea area (such as Bohai Sea), especially in the place where the diffusion coefficient varies greatly in space.

Acknowledgements

This work was funded by the National Natural Science Foundation of China (Nos. 41176007 and 40706007). It was carried out while H. Wang was visiting the Center for Marine Environmental Studies at Ehime University, Japan. She thanks the China Scholarship Council (CSC) for supporting her stay in Japan.

Reference

- Blumberg, A. F., 2002. *A Primer for ECOMSED User Manual (version 1.3)*. HydroQual Inc., Mahwah, New Jersey, 29-31.
- Bolin, B., and Rodhe, H., 1973. A note on the concepts of age distribution and transit time in natural reservoirs. *Tellus*, **25** (1): 58-62, DOI: 10.1111/j.2153-3490.1973.tb01594.x.
- Chen, X., 2007. A laterally averaged two-dimensional trajectory model for estimating transport time scales in the Alafia River estuary, Florida. *Estuarine, Coastal and Shelf Science*, **75** (3): 358-370, DOI: 10.1016/j.ecss.2007.04.020.
- de Brye, B., de Brauwere, A., Gourgue, O., Delhez, E. J. M., and Deleersnijder, E., 2013. Reprint of Water renewal time-scales in the Scheldt Estuary. *Journal of Marine Systems*, **128**: 3-16, DOI: 10.1016/j.jmarsys.2012.03.002.
- Deleersnijder, E., Campin, J. M., and Delhez, E. J. M., 2001. The concept of age in marine modelling I. Theory and preliminary model results. *Journal of Marine Systems*, **28** (3-4): 229-267, DOI: 10.1016/S0924-7963(01)00026-4.
- Delhez, E. J. M., Heemink, A. W., and Deleersnijder, E., 2004. Residence time in a semi-enclosed domain from the solution of an adjoint problem. *Estuarine, Coastal and Shelf Science*, **61** (4): 691-702, DOI: 10.1016/j.ecss.2004.07.013.
- Hilton, A. B. C., McGillivray, D. L., and Adams, E. E., 1998. Residence time of freshwater in Boston's inner harbor. *Journal of Waterway, Port, Coastal, and Ocean Engineering*, **124** (2): 82-89, DOI: 10.1061/(ASCE)0733-950x.
- Liu, W. C., Chen, W. B., and Hsu, M. H., 2011. Using a three-dimensional particle-tracking model to estimate the residence time and age of water in a tidal estuary. *Computers & Geosciences*, **37** (8): 1148-1161, DOI:10.1016/j.cageo.2010.07.007.
- Liu, Z., Wang, H., Guo, X., Wang, Q., and Gao, H., 2012. The age of Yellow River water in Bohai Sea. *Journal of Geophysical Research*, **117**: 1-19, DOI: 10.1029/2012JC008263.
- Monsen, N. E., Cloern, J. E., Lucas, L. V., and Monismith, S. G., 2002. A comment on the use of flushing time, residence time, and age as transport time scales. *Limnology and Oceanography*, **47** (5): 1545-1553, DOI: 10.4319/lo.2002.47.5.1545.
- Takeoka, H., 1984. Fundamental concepts of exchange and transport time scales in a coastal sea. *Continental Shelf Research*, **3** (3): 311-326, DOI: 10.1016/0278-4343(84)90014-1.
- Visser, A. W., 1997. Using random walk models to simulate the vertical distribution of particles in a turbulent water column. *Marine Ecology Progress Series*, **158**: 275-281, DOI: 10.3354/meps158275.
- Wang, Q., Guo, X., and Takeoka, H., 2008. Seasonal variations of the Yellow River plume in Bohai Sea: A model study. *Journal of Geophysical Research*, **113**: 1-14, DOI: 10.1029/2007JC004555.
- Wang, Y., Shen, J., and He, Q., 2010. A numerical model study of the transport timescale and change of estuarine circulation due to waterway constructions in the Changjiang Estuary, China. *Journal of Marine Systems*, **82** (3): 154-170, DOI: 10.1016/j.jmarsys.2010.04.012.
- Zhang, X. Y., 1995. Ocean outfall modeling—Interfacing near and far field models with particle tracking method. PhD thesis. Massachusetts Institute of Technology, Cambridge, 84-109.
- Zimmerman, J. T. F., 1976. Mixing and flushing of tidal embayments in the western Dutch Wadden Sea, Part I: Distribution of salinity and calculation of mixing time scales. *Netherlands Journal of Sea Research*, **10** (4): 149-191, DOI: 10.1016/0077-7579(76)90013-2.

(Edited by Xie Jun)